PAPER

Check for updates

A high-resolution natural abundance ^{33}S MAS NMR study of the cementitious mineral ettringite

Akiko Sasaki,[a] Luis Baquerizo Ibarra[b] and Stephen Wimperis [ID] *[c]

Despite the widespread occurrence of sulfur in both natural and man-made materials, the ^{33}S nucleus has only rarely been utilised in solid-state NMR spectroscopy on account of its very low natural abundance (0.76%), low NMR frequency (ν_0 = 30.7 MHz at B_0 = 9.4 T), and significant nuclear quadrupole moment (spin I = 3/2, Q = −69.4 mb). Satellite-transition magic angle spinning (STMAS) is an NMR method for obtaining high-resolution spectra of half-integer quadrupolar nuclei (spin I > 1/2) in solids and is notable for its intrinsic sensitivity advantage over the similar multiple-quantum (MQMAS) method, especially for nuclei with low NMR frequencies. In this work we demonstrate the feasibility of natural abundance ^{33}S STMAS NMR experiments at B_0 = 9.4 T and 20.0 T using a model sulfate sample (Na_2SO_4 + K_2SO_4 in a 1 : 1 molar ratio). Furthermore, we undertook a natural abundance ^{33}S STMAS NMR study of the cement-forming mineral ettringite ($Ca_6Al_2(SO_4)_3(OH)_{12} \cdot 26H_2O$) at B_0 = 9.4 T and 20.0 T, resolving a discrepancy in the literature between two previous conventional ^{33}S MAS NMR studies and obtaining an alternative set of ^{33}S NMR parameters that is simultaneously consistent with the MAS and STMAS data at both field strengths.

Introduction

Although sulfur is widespread in both nature and materials science, solid-state ^{33}S NMR spectroscopy has been relatively little used as a technique. This is largely due to the low natural abundance of ^{33}S nuclei (0.76%), combined with the high cost of isotopic enrichment, especially where this also involves finding new synthetic routes. In addition, with respect to its gyromagnetic ratio γ, ^{33}S can be categorised as a low-γ nucleus (NMR frequency ν_0 = 30.7 MHz at B_0 = 9.4 T).[1] Since the intrinsic sensitivity of NMR signals is proportional to $\gamma^{5/2}$, this makes obtaining an acceptable signal-to-noise (S/N) ratio difficult. Furthermore, ^{33}S is a half-integer quadrupolar nucleus (spin I = 3/2) and its NMR spectrum is subject to anisotropic broadenings arising from quadrupolar interactions, where the additional linewidth is characterised by a coupling constant, $C_Q = e^2qQ/h$, and asymmetry parameter, $\eta = (V_{xx} - V_{yy})/V_{zz}$. The presence of a quadrupolar interaction thus greatly increases the S/N problems. Recently, however, high-field NMR spectrometers have been employed to advantage to overcome some of the limitations associated with low-γ quadrupolar nuclei. Not only does the intrinsic NMR sensitivity increase at higher magnetic fields but

also there is a significant reduction in the linewidth arising from the second-order quadrupolar broadenings (proportional to $1/\nu_0$). Therefore, with the increasing use of high-field (B_0 > 14.1 T) solid-state NMR spectrometers, solid-state ^{33}S NMR now shows greater potential for future applications.

Solid-state ^{33}S NMR investigations have been relatively scarce in the literature and it seems that only conventional ("one-dimensional") spectra have been reported to date.[1–26] Most of these ^{33}S NMR studies were performed with the ^{33}S nuclei at natural abundance, strongly reflecting the obstacles associated with ^{33}S isotopic enrichment. The earliest solid-state ^{33}S NMR studies date back to 1968 and the immediately ensuing investigations were performed exclusively on sulfides.[2–6,8] In 1986, Eckert and Yesinowski[7] reported an extensive study of "static" solid-state ^{33}S NMR spectra recorded at B_0 = 11.7 T from a total of 27 inorganic compounds including sulfides, sulfates and alums. The first ^{33}S MAS NMR spectra were reported in 1996.[10] In this study, natural abundance ^{33}S MAS NMR spectra of sulfides, sulfates and alums were recorded at B_0 = 14.1 T and this was followed by further ^{33}S MAS NMR studies of sulfides[11] and sulfates[12] recorded at B_0 = 17.6 T and thiosulfates at B_0 = 14.1 T.[13] Satellite-transition spinning sideband manifolds have been observed at B_0 = 14.1 T, where the temperature dependence and a sign change in C_Q were investigated in two alums,[14] while extraction of unambiguous ^{33}S chemical shift anisotropy (CSA) parameters has been achieved for two tetrathiometallates.[16] These mainly medium-field ^{33}S MAS NMR studies were focused on the investigation of simple inorganic compounds owing to

[a] *School of Chemistry and WestCHEM, University of Glasgow, Glasgow G12 8QQ, UK*
[b] *LafargeHolcim Research Centre, 95 Rue du Montmurier, 38070 Saint-Quentin-Fallavier, France*
[c] *Department of Chemistry, Faraday Building, Lancaster University, Lancaster LA1 4YB, UK. E-mail: s.wimperis@lancaster.ac.uk*

the relative ease of recording NMR spectra of S sites in highly symmetric environments with small quadrupolar broadenings. For anhydrous sulfates, long T_1 relaxation times have been reported as an additional limiting factor,[11,12] hampering efficient signal averaging to achieve reasonable S/N ratios for spectral analysis.

During the last decade, the development of sensitivity enhancement techniques for half-integer quadrupolar nuclei and the widespread use of high-field spectrometers have been expanding the use of solid-state ^{33}S NMR as a reliable tool for structural investigations. One of the first high-field ^{33}S NMR studies was carried out at $B_0 = 19.6$ T on cementitious materials containing ^{33}S nuclei as sulfates.[15] Central-transition (CT) enhancement techniques *via* population transfer have been successfully implemented in ^{33}S NMR,[17,19] and observation of three crystallographically distinct S sites in ettringite with C_Q values of up to 1 MHz was possible at $B_0 = 14.1$ T. The Carr–Purcell–Meiboom–Gill (CPMG) pulse sequence is known to boost the S/N ratio by accumulating signal intensity into "spikelets" and, following its success in signal enhancement of ^{33}S-enriched disordered silicates,[18] the CPMG pulse sequence has been frequently employed in high-field solid-state ^{33}S NMR, especially where only a single S site is present.[20–22,24–26] For example, acquisition using the CPMG pulse sequence at $B_0 = 21.1$ T has enabled the observation of large C_Q values (9 to 16 MHz) for a single S site at natural ^{33}S abundance.[22,24] First-principles calculations of ^{33}S NMR parameters accompany many of the latest solid-state ^{33}S NMR studies[20,22–26] to predict and guide assignment of the experimental spectra. Prior knowledge of the magnitudes of quadrupolar broadenings, combined with acquisition at high B_0 fields, has been expanding the range of materials accessible for study by experimental solid-state ^{33}S NMR. For example, a very large C_Q value of 43 MHz was predicted and experimentally observed in elemental sulfur (S_8), owing to the combination of ^{33}S isotopic enrichment, CPMG sensitivity enhancement and first-principles NMR calculations.[23]

In solid-state NMR spectroscopy of half-integer quadrupolar nuclei with overlapping quadrupolar-broadened lineshapes, high-resolution methods such as dynamic angle spinning (DAS),[27] double rotation (DOR),[28] multiple-quantum magic angle spinning (MQMAS),[29] and satellite-transition magic angle spinning (STMAS)[30] NMR experiments are often performed for complete spectral analysis. While the DAS and DOR methods require specialist probes, MQMAS and STMAS are performed using conventional MAS probes. Owing to its robustness and ease in implementation, MQMAS has been applied to investigations of a wide variety of materials containing half-integer quadrupolar nuclei.[31] The STMAS method, on the contrary, is known to be more difficult to implement,[32] owing to experimental requirements such as a stable spinning frequency, accurate setting of the spinning axis to the magic angle, and the virtual necessity of a pneumatic insert and eject system for MAS rotors. One area where MQMAS has had limited applications is in the study of low-γ quadrupolar nuclei, where the required high radiofrequency field strengths (ν_1) are intrinsically difficult to achieve. The sensitivity of the MQMAS method is known to decrease considerably unless high

ν_1 field strengths are employed for the reconversion of multiple- to single-quantum coherences.[33] Largely owing to the single-quantum nature of satellite transitions, STMAS exhibits an inherent sensitivity advantage over MQMAS and relative enhancement factors of three or more are commonly observed for NMR-sensitive nuclei such as ^{23}Na, ^{87}Rb ($I = 3/2$) and ^{27}Al ($I = 5/2$).[33] Previously, the suitability of the STMAS method in preference to MQMAS for the study of low-γ nuclei has been demonstrated,[34] using numerical calculations and ^{39}K ($I = 3/2$, $\nu_0 = 18.7$ MHz at $B_0 = 9.4$ T, 93% natural abundance) and ^{25}Mg ($I = 5/2$, $\nu_0 = 24.5$ MHz at $B_0 = 9.4$ T, 10% natural abundance) STMAS experiments at $B_0 = 9.4$ T. Therefore, it is tempting to investigate what can be achieved using STMAS by means of an extreme case study, such as ^{33}S NMR at the natural ^{33}S abundance of 0.76%.

The purpose of this paper is to demonstrate the feasibility of natural abundance ^{33}S STMAS NMR experiments at $B_0 = 9.4$ T and 20.0 T under favourable conditions. We discuss the technicalities with respect to successful implementation of ^{33}S STMAS experiments at ^{33}S natural abundance before applying the STMAS method to the NMR investigation of the cementitious mineral, ettringite. Ettringite ($Ca_6Al_2(SO_4)_3(OH)_{12} \cdot 26H_2O$) is a hydrous sulfate that is found naturally and also synthetically during the production of cements. Its crystal structure is known from diffraction studies,[35–38] and ^{27}Al MAS NMR studies[39] have been reported previously. There have been two previous ^{33}S solid-state NMR studies of ettringite,[15,17] both at natural isotopic abundance: one at a field $B_0 = 19.6$ T and using conventional single-pulse acquisition[15] and the other at $B_0 = 14.1$ T and employing CT enhancement techniques.[17] These two studies disagree as to the number of crystallographically distinct S sites observed: the higher field study simulates a spectrum with a single S site[15] while the lower field study suggests three S sites[17] in accordance with the diffraction studies. Our aim is to apply the high-resolution ^{33}S STMAS method to ettringite and resolve the ambiguity over the number of crystallographically different S sites observed by solid-state ^{33}S NMR.

Materials and experimental methods

Na_2SO_4, K_2SO_4 and $AlNH_4(SO_4)_2 \cdot 12H_2O$ were obtained commercially as powdered solids and used as received. Ettringite was synthesised from analytical grade reagents. The main precursor in the synthesis of ettringite was tricalcium aluminate ($3CaO \cdot Al_2O_3$), which was prepared from a 3 : 1 molar ratio of $CaCO_3$ and Al_2O_3 at 1400 °C. Anhydrite $CaSO_4$ was prepared by dehydration of gypsum in a muffle furnace at 550 °C overnight. Ettringite was then prepared by suspending a 1 : 3 molar mixture of tricalcium aluminate and anhydrite $CaSO_4$, respectively, with a water-to-solid ratio of 20 using double-distilled CO_2-free water. The mixture was stirred using a magnetic stirrer for three days and then periodically agitated over the period of a fortnight. Once purity was confirmed by X-ray diffraction, the solid was vacuum filtered under an N_2 atmosphere in a glove box and subsequently aged at 25 °C for two months inside hermetic glass bottles equilibrated at 8% relative humidity using a NaOH-saturated salt solution.[40]

^{33}S MAS NMR spectra were acquired at Larmor frequencies (ν_0) of 30.7 and 65.2 MHz using Bruker Avance spectrometers equipped with B_0 = 9.4 and 20.0 T magnets, respectively. Powdered samples were packed into either 4 mm or 7 mm MAS rotors and conventional Bruker MAS probes were employed. Spinning frequencies (ν_R) of 14 286 and 5000–6400 Hz were used with 4 mm and 7 mm rotors, respectively. Single-pulse and rotor-synchronised spin-echo experiments were used to record one-dimensional ^{33}S MAS spectra. The use of ^{1}H decoupling was investigated and found to be unnecessary. The ^{33}S chemical shift scales are given with respect to neat CS$_2$, calibrated using AlNH$_4$(SO$_4$)$_2$·12H$_2$O as a secondary reference (δ_{iso} = 331 ppm).[12] Spectral fitting and simulations of one-dimensional ^{33}S MAS spectra were performed using Bruker TopSpin 3.2. Simulated two-dimensional ^{33}S STMAS spectra and the corresponding isotropic projections were generated in the frequency domain using a home-written Fortran code. Further experimental and computational details are provided in the figure captions.

A powdered mixture of Na$_2$SO$_4$ and K$_2$SO$_4$ was packed into a 4 mm MAS rotor, while powdered ettringite was packed into a 7 mm rotor. The most efficient manipulation of satellite-transition (ST) coherences is achieved with high radiofrequency field strengths and, as has been shown previously, this can result in a smaller diameter rotor producing the highest STMAS sensitivity, with the beneficial effects of the higher ν_1 frequency outweighing those of the reduced sample volume.[34] However, after concluding our preliminary experiments with the mixture of Na$_2$SO$_4$ and K$_2$SO$_4$, we discovered that the ν_1 frequencies yielded by the 4 mm and (single-channel) 7 mm MAS probes on the 20.0 T spectrometer were similar and so we used a 7 mm rotor for all the ettringite experiments at both B_0 = 9.4 and 20.0 T. Obviously, whatever the rotor diameter, the use of the highest radiofrequency power available is recommended for the efficient manipulation of ST coherences, i.e., for the first two pulses in the STMAS pulse sequence. In our work, the 1 kW amplifiers produced ^{33}S radiofrequency field strengths (ν_1 = $|\gamma B_1|/2\pi$) estimated to be around 55 kHz on both the 9.4 T and 20.0 T instruments.

The phase-modulated split-t_1 STMAS pulse sequence[32,41] was used in all the ^{33}S STMAS experiments in this study as it seems to be the most sensitive basic implementation of the technique.[32,34] For sensitive NMR nuclei (such as ^{23}Na, ^{87}Rb and ^{27}Al), it is possible to optimise the durations of each pulse experimentally and obtain the highest S/N ratio on the sample of interest. However, for low sensitivity nuclei such as ^{33}S it is impractical to perform such pulse length optimisations unless ^{33}S-enriched samples suitable for STMAS experiments are available (and generally these will not be, as they were not to us). Previously, numerical calculations[34] have shown that, for spin I = 3/2, the optimum flip angles for the first ST excitation pulse (p1) and second ST reconversion pulse (p2) are 90° and 60°, respectively; the third pulse (p3) is a CT-selective "180°" inversion pulse, as in the second pulse of the spin-echo sequence. It should be noted that the flip angles quoted for the first two STMAS pulses are intrinsic values; e.g., the values of $2\pi\nu_1\tau_{p1}$ and $2\pi\nu_1\tau_{p2}$. In contrast, the third pulse is a "soft" inversion or refocusing pulse that acts only on the central transition and, for I = 3/2, has an intrinsic flip angle of 90°, with the selective nutation rate increased by a factor of $I + 1/2$. Our approach is then to calibrate the ^{33}S radiofrequency field strength and then to calculate the corresponding STMAS pulse durations.[34] For the calibration we employed the ^{33}S MAS NMR signal of AlNH$_4$(SO$_4$)$_2$·12H$_2$O. The negligible value of C_Q (resulting in linewidth at half height of 18 Hz) and short T_1 relaxation time (0.27 s)[12] of this solid makes it ideal as a setup sample for ^{33}S MAS experiments.[1] For the first two STMAS pulses, the maximum available ^{33}S radiofrequency field strength (ν_1) of 55 kHz was employed, while for the CT-selective 180° pulse, ν_1(^{33}S) = 15 kHz was appropriate. The actual pulse lengths used for p1, p2 and p3 were 4.5, 3.0 and 17.0 μs, respectively, in all our ^{33}S STMAS experiments.

It is well known that a double-quantum filtered (DQF) version of the STMAS pulse sequence simplifies the resulting spectrum by the removal of the CT–CT autocorrelation peaks.[42] However, excitation of double-quantum coherences is inefficient for spins with small C_Q values[32] (<1 MHz for I = 3/2 nuclei, for example), as we are expecting with ^{33}S. Furthermore, since for I = 3/2 the optimum flip angle of 90° for the ST excitation pulse (p1) corresponds to a CT-selective "180°", the CT–CT autocorrelation peaks are anticipated to be of low intensity even without use of a double-quantum filter. For this reason, the basic phase-modulated split-t_1 STMAS experiment and not the DQF-STMAS sequence was used for the ^{33}S NMR experiments in this work.

In STMAS, accurate setting of sample spinning axis to 54.736 ± 0.002° is a prerequisite.[32] Prior to our ^{33}S STMAS experiments, phase-modulated split-t_1 ^{85}Rb (spin I = 5/2) DQF-STMAS experiments[42] were performed on RbNO$_3$ for accurate spinning axis calibration. There are several advantages associated with the use of ^{85}Rb DQF-STMAS experiments performed on RbNO$_3$: ^{85}Rb is easily observable (72% natural abundance), the ^{85}Rb Larmor frequency is close enough to ^{33}S to lie within the same tuning range of an MAS probe (ν_0(^{85}Rb) = 38.6 MHz and ν_0(^{33}S) = 30.7 MHz at B_0 = 9.4 T), efficient ^{85}Rb spin–lattice relaxation ($T_1 \approx$ 60 ms)[43] saves considerable time during the stepwise adjustment of the spinning axis, the magnitude of the ^{85}Rb quadrupolar interactions is large enough (P_Q = 3.7–4.7 MHz)[44] to observe the effect of angle misset easily, and the DQF version of the STMAS pulse sequence (which works well here) simplifies the resulting spectrum by the removal of CT–CT autocorrelation peaks.[42] In practice, we record a one-dimensional DQF-STMAS spectrum, corresponding to a single t_1 value and maximise the signal amplitude, followed by acquisition of full two-dimensional DQF-STMAS spectra to ensure the removal of any residual splitting arising from spinning angle misset. Residual splittings due to third-order quadrupolar interactions can be significant for I = 5/2 nuclei such as ^{85}Rb (but note that they are insignificant for I = 3/2 nuclei such as ^{33}S) and their presence should be taken into account, especially at lower B_0 fields as they are proportional to $1/\nu_0^2$.[32,45]

Once the magic angle is achieved with the RbNO$_3$ setup sample, changing the sample, even using the Bruker pneumatic insert-eject system, has the potential to alter the spinning angle if not performed carefully. On the B_0 = 9.4 T spectrometer,

Table 1 Experimental [33]S NMR parameters for sodium sulfate and potassium sulfate taken from ref. 26 and this work (Fig. 2). The magnetic field dependent shifts δ_1 and δ_2 were measured at $B_0 = 20.0$ T. The P_Q values in brackets were calculated from the C_Q and η values in ref. 26 for comparison with the values determined in this work

	δ_{iso} (ppm)	C_Q (kHz)	η	δ_1 (ppm)	δ_2 (ppm)	P_Q (kHz)
Na$_2$SO$_4$						
Ref. 26	340.1 ± 1.0	655 ± 50	0.0 ± 0.1			(655 ± 50)
This work (Fig. 2)	340.6 ± 0.5			342.1 ± 0.5	338.1 ± 0.5	650 ± 80
K$_2$SO$_4$						
Ref. 26	335.7 ± 0.5	959 ± 30	0.42 ± 0.05			(988 ± 37)
This work (Fig. 2)	336.4 ± 0.7			339.8 ± 0.5	330.6 ± 1.0	990 ± 80

we used a low flow of bearing or eject gas to cushion the rotor during the insertion. However, with a 7 mm rotor on the $B_0 = 20.0$ T magnet this still produced a change in the spinning angle, perhaps due to the greater height that the rotor has to fall in the larger magnet. Consequently, a layer of RbNO$_3$ was added to the powdered ettringite for experiments at $B_0 = 20.0$ T, thus avoiding the ejection and insertion procedure normally associated with the spinning axis calibration. To maximise the [33]S sensitivity, powdered RbNO$_3$ was first packed into the bottom of a 7 mm rotor (about 20% of the total volume) and the rest of the rotor was filled with the ettringite. Upon comparison of two [33]S MAS spectra, one recorded with a 7 mm rotor full of ettringite and one recorded with a 7 mm rotor also containing RbNO$_3$ at the bottom, the resulting [33]S MAS spectra were confirmed to be identical except for a small difference in sensitivity proportional to the sample volume inside each rotor.

At $B_0 = 20.0$ T, we acquired [33]S spin-echo MAS spectra of ettringite with various intervals between the two pulses (3–12 ms) to determine the optimum length of the echo interval in the
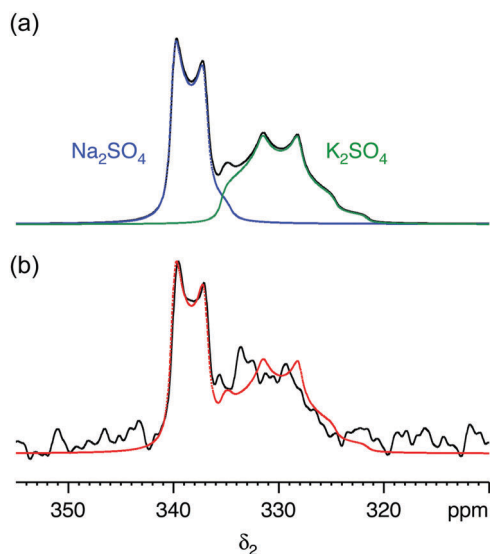

Fig. 2 (a) Simulated and (b) experimental [33]S STMAS spectra of a 1:1 molar mixture of sodium sulfate (Na$_2$SO$_4$) and potassium sulfate (K$_2$SO$_4$) at $B_0 = 20.0$ T, with the corresponding isotropic projections. In (a) the [33]S NMR parameters (δ_{iso}, C_Q and η) were taken from ref. 26 (see Table 1). In (b) 192 transients were averaged for each of 67 t_1 increments of 132.22 μs with a relaxation interval of 20 s. An echo interval (τ) of 12 ms was used. Total experimental time was 72 h. The MAS frequency was 14 286 Hz. A 4 mm MAS rotor was used. Contour levels are drawn at 16, 32, 48, 64, 80, and 96% of the maximum value. No weighting functions were applied in (b).

Fig. 1 (a) Simulated and (b) experimental [33]S MAS spectra of a 1:1 molar mixture of sodium sulfate (Na$_2$SO$_4$) and potassium sulfate (K$_2$SO$_4$) at $B_0 = 20.0$ T. In (a) the [33]S NMR parameters (δ_{iso}, C_Q and η) were taken from ref. 26 (see Table 1). In (b) a spin-echo pulse sequence was used. The MAS frequency was 14 286 Hz. A 4 mm MAS rotor was used. 4928 transients were averaged with a relaxation interval of 30 s. Total experimental time was 41 h. The complete simulated lineshape from (a) is overlaid (red) on the experimental lineshape (black).
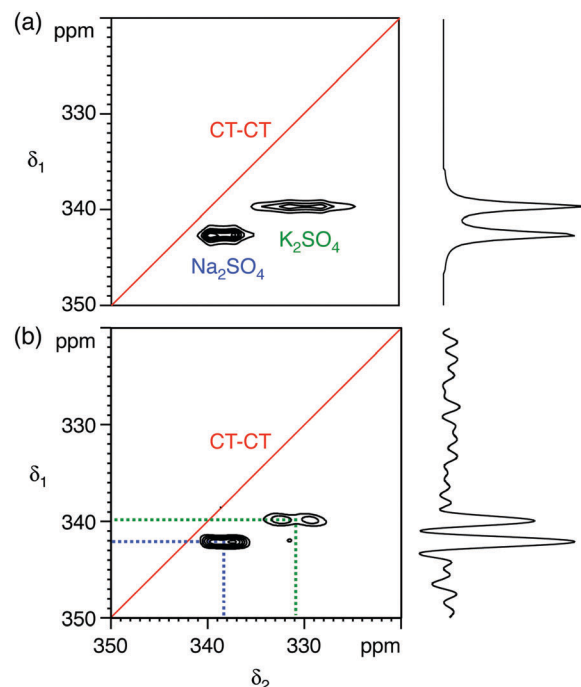
Table 2 Experimental [33]S NMR parameters for ettringite taken from ref. 15 and 17 and this work (Fig. 3 and 4). The magnetic field dependent isotropic shifts δ_1 in brackets were calculated at $B_0 = 9.4$ T and $B_0 = 20.0$ T from the C_Q and η values given in ref. 15 and 17 and determined in this work to allow comparison with the experimental STMAS spectra

	δ_{iso} (ppm)	C_Q (kHz)	η	δ_1 at 9.4 T (ppm)	δ_1 at 20.0 T (ppm)
Ref. 15	331	700	0.45	(339.2)	(332.8)
Ref. 17	331.1	516 ± 5	0.50 ± 0.05	(335.6)	(332.1)
	329.8	591 ± 5	0.72 ± 0.05	(336.2)	(331.2)
	329.6	810 ± 5	0.97 ± 0.05	(343.0)	(332.6)
This work (Fig. 3 and 4)	331.8	620 ± 20	0.1 ± 0.1	337.8	(333.1)
	332.1	660 ± 20	0.3 ± 0.1	339.1	(333.7)
	331.0	800 ± 20	0.1 ± 0.1	341.0	(333.2)

This journal is © the Owner Societies 2017

Phys. Chem. Chem. Phys., 2017, **19**, 24082–24089 | 24085

STMAS sequence, attempting to avoid truncation of STMAS signals while retaining sensitivity; a value of 12 ms was used in our experiments. At B_0 = 9.4 T, a short echo interval (4 ms) was employed for maximum sensitivity (the optimum is possibly longer than 8 ms but the effect of signal truncation was not obvious in the resulting spectrum due to the low S/N ratio).

Results and discussion

We first demonstrate the feasibility of natural abundance ^{33}S STMAS experiments on a model system with known and undisputed NMR parameters, a 1:1 molar mixture of Na_2SO_4 and K_2SO_4, with experiments performed at B_0 = 20.0 T. The ^{33}S MAS spectrum of each sulfate has been reported previously,[12,17,26]
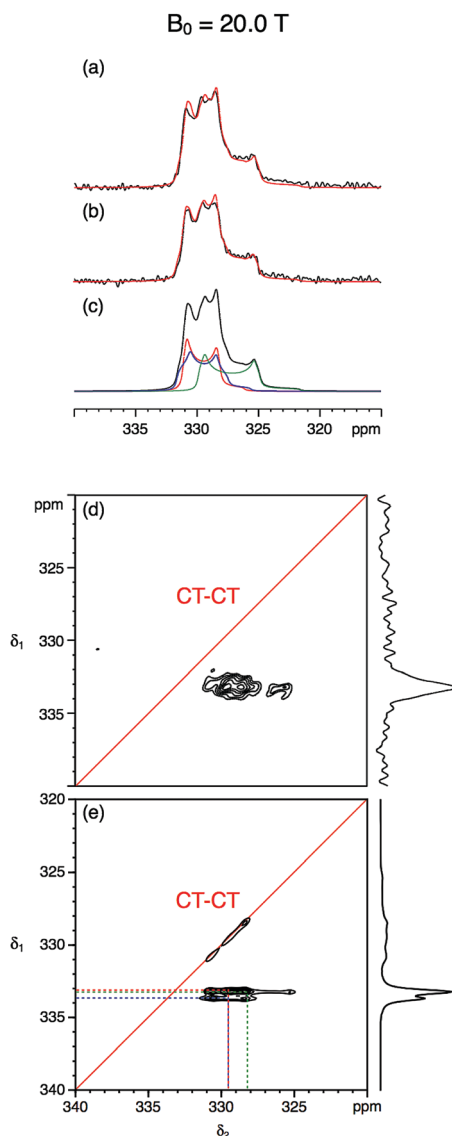

Fig. 3 (a–c) Experimental and simulated ^{33}S MAS and (d and e) experimental and simulated STMAS spectra of ettringite with corresponding isotropic projections at B_0 = 20.0 T. In (a) a single pulse and (b) a spin-echo pulse sequence was used. In both (a) and (b) 92 160 transients were averaged with a relaxation interval of 0.6 s. Total experimental time was 16 h in each case. The MAS frequency was 6.4 kHz. A 7 mm MAS rotor filled only with ettringite was used. No weighting functions were applied. (c and e) Simulated ^{33}S MAS and STMAS spectra using the NMR parameters (δ_{iso}, C_Q and η) determined in this work and given in Table 2. In (d) 11 040 transients were averaged for each of 64 t_1 increments of 377.78 μs with a relaxation interval of 0.45 s. An echo interval (τ) of 6 ms was used. Total experimental time was 92 h. The MAS frequency was 5 kHz. A 7 mm MAS rotor containing both RbNO$_3$ and ettringite was used. Contour levels are drawn at 32, 44, 56, 68, 80, and 92% of the maximum value. No weighting functions were applied.
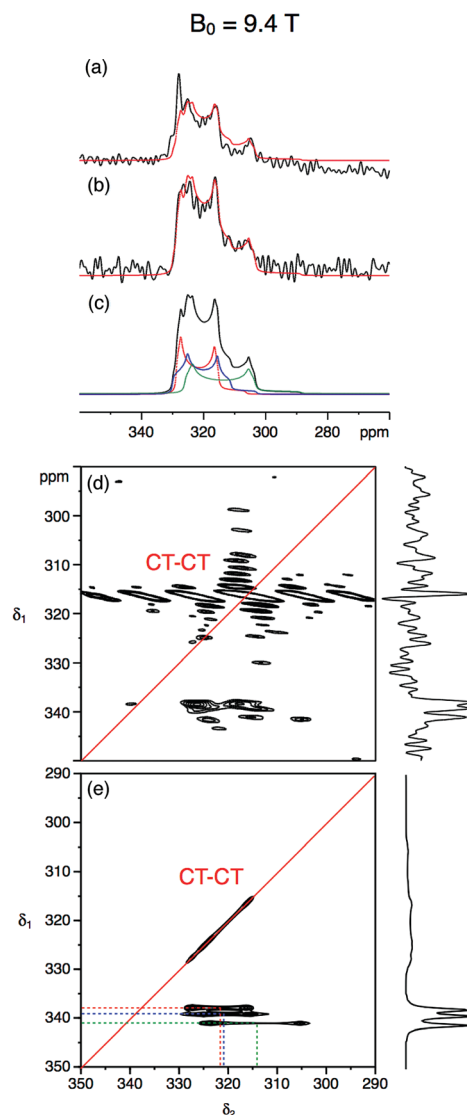
Fig. 4 (a–c) Experimental and simulated ^{33}S MAS and (d and e) experimental and simulated STMAS spectra of ettringite with corresponding isotropic projections at B_0 = 9.4 T. In (a) a single pulse and (b) a spin-echo pulse sequence was used. In both (a) and (b), 524 288 transients were averaged with a relaxation interval of 0.25 s. Total experimental time was 44 h in each case. The MAS frequency was 6.4 kHz. A 7 mm MAS rotor filled only with ettringite was used. No weighting functions were applied. (c and e) Simulated ^{33}S MAS and STMAS spectra using the NMR parameters (δ_{iso}, C_Q and η) determined in this work and given in Table 2. In (d) 40 960 transients were averaged for each of 85 t_1 increments of 295.14 μs with a relaxation interval of 0.25 s. An echo interval (τ) of 4 ms was used. Total experimental time was 262 h. The MAS frequency was 6.4 kHz. A 7 mm MAS rotor filled only with ettringite was used. Contour levels are drawn at 32, 44, 56, 68, 80, and 92% of the maximum value. No weighting functions were applied.

24086 | *Phys. Chem. Chem. Phys.*, 2017, **19**, 24082–24089

This journal is © the Owner Societies 2017

and the ^{33}S NMR parameters from ref. 26 are summarised in Table 1. Both sulfates have similar isotropic chemical shifts (δ_{iso} shifts of 340 ppm and 336 ppm) and small quadrupolar broadenings (C_Q coupling constants of 0.655 MHz and 0.988 MHz). Our simulated ^{33}S MAS spectrum of the equimolar sulfate mixture at B_0 = 20.0 T (Fig. 1a) indicates the presence of overlapping second-order broadened lineshapes and this was confirmed by the experimental ^{33}S MAS spectrum of the sulfate mixture at B_0 = 20.0 T shown in Fig. 1b. A simulated ^{33}S STMAS spectrum of the sulfate mixture at B_0 = 20.0 T using quadrupolar parameters previously reported for each sulfate is shown in Fig. 2a. The two STMAS ridges are expected to be resolved in the δ_1 (isotropic) dimension and this was confirmed by our experimental natural abundance ^{33}S STMAS spectrum of the sulfate mixture recorded at B_0 = 20.0 T, shown in Fig. 2b. A total acquisition time of three days was required to obtain this spectrum, although the major limiting factor here was the long T_1 relaxation times of these anhydrous sulfates (T_1 = 30 s for Na$_2$SO$_4$ and 16 s for K$_2$SO$_4$).[12] The poor S/N in the δ_2 cross sections from Fig. 2b made any lineshape fitting unreliable but, using the δ_1 and δ_2 peak positions in the two-dimensional STMAS spectrum, a centre-of-mass analysis was carried out using the appropriate equations for I = 3/2 split-t_1 STMAS experiments to obtain the isotropic chemical shift, δ_{iso}, and the isotropic I = 3/2 second-order quadrupolar shift, $\delta_Q = (250 C_Q/\nu_0)^2 (1 + \eta^2/3)$:[32,34]

$$\delta_{iso} = (17\delta_1 + 10\delta_2)/27 \tag{1a}$$

$$\delta_Q = 85(\delta_1 - \delta_2)/54 \tag{1b}$$

The isotropic I = 3/2 quadrupolar shift was then used to obtain the composite quadrupolar product $P_Q = C_Q (1 + (\eta^2/3))^{1/2}$:

$$P_Q = \frac{\nu_0 \sqrt{\delta_Q}}{250} \tag{2}$$

This procedure yielded the chemical shift and quadrupolar parameters summarised in Table 1, which are in satisfactory agreement with the previously reported NMR parameters.

Following on from this successful feasibility study, our investigations of ettringite in a 7 mm MAS rotor using natural abundance ^{33}S NMR were conducted at, initially, B_0 = 20.0 T and, subsequently, B_0 = 9.4 T. A set of three experiments (single-pulse, spin-echo, and STMAS) was performed each field strength. Previously, two studies reported natural abundance ^{33}S MAS spectra of ettringite,[15,17] one at B_0 = 19.6 T using conventional single-pulse acquisition,[15] and the other at B_0 = 14.1 T employing CT enhancement techniques.[17] The higher B_0 field study simulates a spectrum with a single site[15] while the lower B_0 field study proposes three S sites[17] in accordance with the diffraction studies. The chemical shift and quadrupolar parameters determined in these two studies are summarised in Table 2. Both studies employed a relaxation interval of 1 s and we have qualitatively verified this very efficient ^{33}S spin–lattice relaxation in ettringite (the use of 0.2 s as a recycle interval gave rise to a 10% loss in sensitivity compared with the use of 0.4 s at B_0 = 20.0 T). It was this efficient relaxation that encouraged us to attempt experiments at the relatively low field strength of B_0 = 9.4 T.

Fig. 3 and 4 show the natural abundance ^{33}S single-pulse, spin-echo and STMAS spectra of ettringite in a 7 mm MAS rotor at B_0 = 20.0 T and 9.4 T, respectively. It is apparent from the B_0 = 20.0 T STMAS spectrum in Fig. 3d, which took 92 h to record, that, although there is some evidence of the presence of more than one two-dimensional lineshape, multiple S sites are not fully resolved. Recognising that this was likely to be the result of small second-order quadrupolar shifts at B_0 = 20.0 T, we were encouraged to record the B_0 = 9.4 T ^{33}S STMAS spectrum of ettringite shown in Fig. 4d, which took 262 h to complete. Although the S/N ratio is poor and there are strong truncation artefacts at $\delta_1 \approx 0$, the δ_1 projection of the spectrum appears to show isotropically resolved S sites.

Centre-of-mass analyses were performed on the two-dimensional STMAS spectra using the appropriate equations for I = 3/2 split-t_1 experiments[34] (eqn (1)–(2)). These provided initial estimates for the chemical shift and quadrupolar parameters for ettringite that were
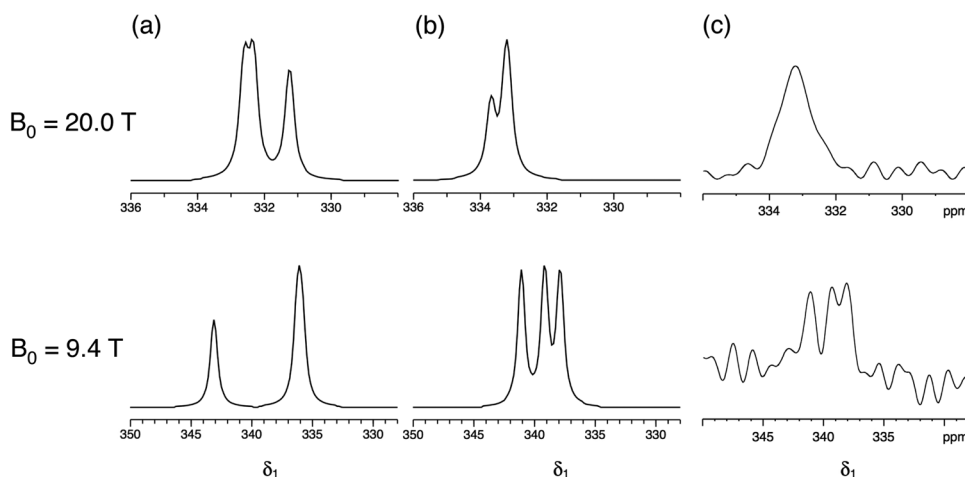

Fig. 5 (a and b) Simulated and (c) experimental isotropic projections of two-dimensional ^{33}S STMAS spectra of ettringite at B_0 = 20.0 T and 9.4 T. ^{33}S NMR parameters (δ_{iso}, C_Q and η) were taken from (a) ref. 17 and (b) this work, as summarised in Table 2.

This journal is © the Owner Societies 2017

Phys. Chem. Chem. Phys., 2017, **19**, 24082–24089 | 24087

then used in an iterative fitting of the one-dimensional MAS spectra at the two field strengths. Further refinement of the NMR parameters was then achieved by comparing the simulated δ_1 projections of the STMAS spectra at the two field strengths with the experimental projections. In this way we obtained a consistent set of chemical shift and quadrupolar parameters at $B_0 = 20.0$ T and 9.4 T for the three crystallographically distinct S sites in ettringite, as summarised in Table 2.

Fig. 5 compares the simulated δ_1 projections at $B_0 = 20.0$ T and 9.4 T using the parameters obtained in this work with those using the parameters from ref. 17 and with the experimental ^{33}S STMAS δ_1 projections. It is apparent that the ^{33}S NMR parameters from ref. 17 do not reproduce the experimental STMAS δ_1 projections obtained in this work. With respect to this, we note that the spectra in ref. 17 were recorded with the assistance of a CT enhancement method, which may have distorted the ^{33}S MAS lineshapes, and were subjected to significant line broadening (up to 50 Hz)[17] during processing.

Conclusions

We have demonstrated the feasibility of high-resolution ^{33}S STMAS NMR experiments at $B_0 = 9.4$ and 20.0 T and at the natural abundance of ^{33}S (0.76%). We judge that, at ^{33}S natural abundance in the presence of multiple S sites, ^{33}S STMAS is feasible at $B_0 = 20.0$ T for quadrupolar coupling constants up to 1 MHz in magnitude. If the ^{33}S spin–lattice relaxation times are particularly short, as in the case of ettringite, then our results indicate that ^{33}S STMAS becomes possible at lower field strengths, such as the $B_0 = 9.4$ T used here. Total acquisition times can be very long, a week or more, and we were fortunate that our $B_0 = 9.4$ T magnet was particularly stable. Using ^{33}S STMAS at ^{33}S natural abundance, we have resolved the disagreement in the ^{33}S NMR literature as to the number of distinct S sites in the mineral ettringite in favour of ref. 17: we also find 3 distinct S sites, in further agreement with diffraction studies. We have obtained a set of ^{33}S NMR parameters (δ_{iso}, C_Q and η) for ettringite that are in consistent agreement with ^{33}S MAS and STMAS spectra recorded at field strengths of $B_0 = 9.4$ and 20.0 T. The importance of working at more than one magnetic field strength cannot be overstated in a challenging study such as that presented here. Finally, we note that the highly dynamic nature of the ettringite structure, as evidenced by the unusually short ^{33}S T_1 relaxation times, is expected to complicate attempts to calculate the ^{33}S NMR parameters using first-principles methods such as WIEN2k or CASTEP, as we have confirmed in preliminary DFT studies.

Conflicts of interest

There are no conflicts to declare.

Acknowledgements

References

1 M. E. Smith, Recent Progress in Solid-State NMR of Low-γ Nuclei, *Annu. Rep. NMR Spectrosc.*, 2001, **43**, 121–175.

2 C. Karr and H. D. Schultz, Wide-Line Nuclear Magnetic Resonance Spectroscopy of Sulfur-33 in Minerals, *Spectrosc. Lett.*, 1968, **1**, 205–210.

3 K. Lee, ^{33}S Nuclear Magnetic Resonance in Paramagnetic α-MnS, *Phys. Rev.*, 1968, **172**, 284–287.

4 H. Suzuki, T. Komaru, T. Hihara and Y. Koi, Nuclear Magnetic Resonances of ^{33}S and ^{77}Se in EuS and EuSe, *J. Phys. Soc. Jpn.*, 1971, **30**, 288.

5 H. L. Retcofsky and R. A. Friedel, Sulfur-33 Magnetic Resonance Spectra of Selected Compounds, *J. Am. Chem. Soc.*, 1972, **94**, 6579–6584.

6 M. Haller, W. E. Hertler, O. Lutz and A. Nolle, ^{67}Zn and ^{33}S Nuclear Shielding in Zinc Chalcogenides, *Solid State Commun.*, 1980, **33**, 1051–1053.

7 H. Eckert and J. P. Yesinowski, Sulfur-33 NMR at Natural Abundance in Solids, *J. Am. Chem. Soc.*, 1986, **108**, 2140–2146.

8 T. J. Bastow and S. N. Stuart, NMR Study of the Zinc Chalcogenides, *Phys. Status Solidi B*, 1988, **145**, 719–728.

9 M. J. Collins, C. I. Ratcliffe and J. A. Ripmeester, 2H and ^{33}S NMR Line-Shape Studies of the Molecular Motion in the Lipid and Solid Phases of Hydrogen Sulfide and the Solid II of Hydrogen Selenide, *J. Phys. Chem.*, 1989, **93**, 7495–7502.

10 W. A. Daunch and P. L. Rinaldi, Natural-Abundance Solid-State ^{33}S NMR with High-Speed Magic-Angle Spinning, *J. Magn. Reson., Ser. A*, 1996, **123**, 219–221.

11 T. A. Wagler, W. A. Daunch, P. L. Rinaldi and A. R. Palmer, Solid State ^{33}S NMR of Inorganic Sulfides, *J. Magn. Reson.*, 2003, **161**, 191–197.

12 T. A. Wagler, W. A. Daunch, M. Panzner, W. J. Youngs and P. L. Rinaldi, Solid-State ^{33}S MAS NMR of Inorganic Sulfates, *J. Magn. Reson.*, 2004, **170**, 336–344.

13 S. Couch, A. P. Howes, S. C. Kohn and M. E. Smith, ^{33}S Solid State NMR of Sulphur Speciation in Silicate Glasses, *Solid State Nucl. Magn. Reson.*, 2004, **26**, 203–208.

14 H. J. Jakobsen, A. R. Hove, H. Bildsøe and J. Skibsted, Satellite Transitions in Natural Abundance Solid-State ^{33}S MAS NMR of Alums – Sign Change with Zero-Crossing of CQ in a Variable Temperature Study, *J. Magn. Reson.*, 2006, **180**, 170–177.

15 J.-B. d'Espinose de Lacaillerie, F. Barberon, B. Bresson, P. Fonollosa, H. Zanni, V. E. Fedorov, N. G. Naumov and

24088 | *Phys. Chem. Chem. Phys.*, 2017, **19**, 24082–24089

This journal is © the Owner Societies 2017

Z. Gan, Applicability of Natural Abundance ^{33}S Solid-State NMR to Cement Chemistry, *Cem. Concr. Res.*, 2006, **36**, 1781–1783.

16 H. J. Jakobsen, A. R. Hove, H. Bildsøe, J. Skibsted and M. Brorson, Advancements in Natural Abundance Solid-State ^{33}S MAS NMR: Characterization of Transition-Metal M=S Bonds in Ammonium Tetrathiometallates, *Chem. Commun.*, 2007, 1629–1631.

17 M. R. Hansen, M. Brorson, H. Bildsøe, J. Skibsted and H. J. Jakobsen, Sensitivity Enhancement in Natural-Abundance Solid-State ^{33}S MAS NMR Spectroscopy Employing Adiabatic Inversion Pulses to the Satellite Transitions, *J. Magn. Reson.*, 2008, **190**, 316–326.

18 L. A. O'Dell, K. Klimm, J. C. C. Freitas, S. C. Kohn and M. E. Smith, ^{33}S MAS NMR of a Disordered Sulfur-Doped Silicate: Signal Enhancement via RAPT, QCPMG and Adiabatic Pulses, *Appl. Magn. Reson.*, 2008, **35**, 247–259.

19 H. J. Jakobsen, H. Bildsøe, J. Skibsted, M. Brorson, B. R. Srinivasan, C. Näther and W. Bensch, New Opportunities in Acquisition and Analysis of Natural Abundance Complex Solid-State ^{33}S MAS NMR Spectra: (CH$_3$NH$_3$)$_2$WS$_4$, *Phys. Chem. Chem. Phys.*, 2009, **11**, 6981–6986.

20 A. Sutrisno, V. V. Terskikh and Y. Huang, A Natural Abundance ^{33}S Solid-State NMR Study of Layered Transition Metal Disulfides at Ultrahigh Magnetic Field, *Chem. Commun.*, 2009, 186–188.

21 H. J. Jakobsen, H. Bildsøe, J. Skibsted, M. Brorson, P. Gor'kov and Z. Gan, A Strategy for Acquisition and Analysis of Complex Natural Abundance ^{33}S Solid-State NMR Spectra of a Disordered Tetrathio Transition-Metal Anion, *J. Magn. Reson.*, 2010, **202**, 173–179.

22 I. Moudrakovski, S. Lang, S. Patchkovskii and J. Ripmeester, High Field ^{33}S Solid State NMR and First-Principles Calculations in Potassium Sulfates, *J. Phys. Chem. A*, 2010, **114**, 309–316.

23 L. A. O'Dell and I. L. Moudrakovski, Testing the Sensitivity Limits of ^{33}S NMR: An Ultra-Wideline Study of Elemental Sulfur, *J. Magn. Reson.*, 2010, **207**, 345–347.

24 P. J. Pallister, I. L. Moudrakovski and J. A. Ripmeester, High-Field Multinuclear Solid-State Nuclear Magnetic Resonance (NMR) and First Principle Calculations in MgSO$_4$ Polymorphs, *Can. J. Chem.*, 2011, **89**, 1076–1086.

25 L. A. O'Dell and C. I. Ratcliffe, Crystal Structure Based Design of Signal Enhancement Schemes for Solid-State NMR of Insensitive Half-Integer Quadrupolar Nuclei, *J. Phys. Chem. A*, 2011, **115**, 747–752.

26 P. J. Pallister, I. L. Moudrakovski, G. D. Enright and J. A. Ripmeester, Structural Assessment of Anhydrous Sulfates with High Field ^{33}S Solid State NMR and First Principles Calculations, *CrystEngComm*, 2013, **15**, 8808–8822.

27 A. Llor and J. Virlet, Towards High-Resolution NMR of More Nuclei in Solids: Sample Spinning with Time-Dependent Spinner Axis Angle, *Chem. Phys. Lett.*, 1988, **152**, 248–253.

28 A. Samoson, E. Lippmaa and A. Pines, High Resolution Solid-State N.M.R, *Mol. Phys.*, 1988, **65**, 1013–1018.

29 L. Frydman and J. S. Harwood, Isotropic Spectra of Half-Integer Quadrupolar Spins from Bidimensional Magic-Angle Spinning NMR, *J. Am. Chem. Soc.*, 1995, **117**, 5367–5368.

30 Z. Gan, Isotropic NMR Spectra of Half-Integer Quadrupolar Nuclei Using Satellite Transitions and Magic-Angle Spinning, *J. Am. Chem. Soc.*, 2000, **122**, 3242–3243.

31 *NMR of Quadrupolar Nuclei in Solid Materials*, ed. R. E. Wasylishen, S. E. Ashbrook and S. Wimperis, John Wiley & Sons, Ltd, Chichester, 2012.

32 S. E. Ashbrook and S. Wimperis, High-Resolution NMR of Quadrupolar Nuclei in Solids: The Satellite-Transition Magic Angle Spinning (STMAS) Experiment, *Prog. Nucl. Magn. Reson. Spectrosc.*, 2004, **45**, 53–108.

33 J. Amoureux, C. Fernandez and L. Frydman, Optimized Multiple-Quantum Magic-Angle Spinning NMR Experiments on Half-Integer Quadrupoles, *Chem. Phys. Lett.*, 1996, **259**, 347–355.

34 N. G. Dowell, S. E. Ashbrook and S. Wimperis, Satellite-Transition MAS NMR of Low-γ Nuclei at Natural Abundance: Sensitivity, Practical Implementation, and Application to ^{39}K (I = 3/2) and ^{25}Mg (I = 5/2), *J. Phys. Chem. B*, 2004, **108**, 13292–13299.

35 A. Moore and H. F. W. Taylor, Crystal Structure of Ettringite, *Nature*, 1968, **218**, 1048–1049.

36 A. E. Moore and H. F. W. Taylor, Crystal Structure of Ettringite, *Acta Crystallogr.*, 1970, **B26**, 386–393.

37 F. Goetz-Neunhoeffer and J. Neubauer, Refined Ettringite (Ca$_6$Al$_2$(SO$_4$)$_3$(OH)$_{12}$·26H$_2$O) Structure for Quantitative X-Ray Diffraction Analysis, *Powder Diffr.*, 2006, **21**, 4–11.

38 M. R. Hartman and R. Berliner, Investigation of the Structure of Ettringite by Time-of-Flight Neutron Powder Diffraction Techniques, *Cem. Concr. Res.*, 2006, **36**, 364–370.

39 J. Skibsted, E. Henderson and H. J. Jakobsen, Characterization of Calcium Aluminate Phases in Cements by ^{27}Al MAS NMR Spectroscopy, *Inorg. Chem.*, 1993, **32**, 1013–1027.

40 L. Greenspan, Humidity Fixed Points of Binary Saturated Aqueous Solutions, *J. Res. Natl. Bur. Stand., Sect. A*, 1977, **81**, 89–96.

41 K. J. Pike, S. E. Ashbrook and S. Wimperis., Two-Dimensional Satellite-Transition MAS NMR of Quadrupolar Nuclei: Shifted Echoes, High-Spin Nuclei and Resolution, *Chem. Phys. Lett.*, 2001, **345**, 400–408.

42 H.-T. Kwak and Z. Gan, Double-Quantum Filtered STMAS, *J. Magn. Reson.*, 2003, **164**, 369–372.

43 J. T. Cheng, J. C. Edwards and P. D. Ellis, Measurement of Quadrupolar Coupling Constants, Shielding Tensor Elements, and the Relative Orientation of Quadrupolar and Shielding Tensor Principal Axis Systems for Rubidium-87 and Rubidium-85 Nuclei in Rubidium Salts by Solid-State Nuclear Magnetic Resonance, *J. Phys. Chem.*, 1990, **94**, 553–561.

44 I. Hung, A. Wong, A. P. Howes, T. Anupõld, A. Samoson, M. E. Smith, D. Holland, S. P. Brown and R. Dupree, Separation of Isotropic Chemical and Second-Order Quadrupolar Shifts by Multiple-Quantum Double Rotation NMR, *J. Magn. Reson.*, 2009, **197**, 229–236.

45 Z. Gan, P. Srinivasan, J. R. Quine, S. Steuernagel and B. Knott, Third-Order Effect in Solid-State NMR of Quadrupolar Nuclei, *Chem. Phys. Lett.*, 2003, **367**, 163–169.

This journal is © the Owner Societies 2017

Phys. Chem. Chem. Phys., 2017, **19**, 24082–24089 | 24089